catalysts

MDPI

Review

Advanced XPS-Based Techniques in the Characterization of Catalytic Materials: A Mini-Review

Yuanyuan Cui [1,*], Yifan Liao [2], Youbao Sun [1], Wenchang Wang [1], Jinqi Wu [1], Weilin Dai [2] and Taohong Huang [1,*]

[1] Shimadzu China Co., Ltd., Shanghai 200233, China
[2] Department of Chemistry, Shanghai Key Laboratory of Molecular Catalysis and Innovative Materials, Fudan University, Shanghai 200433, China; wldai@fudan.edu.cn (W.D.)
* Correspondence: sshcuiyy@163.com (Y.C.); sshhth@shimadzu.com.cn (T.H.)

Abstract: X-ray photoelectron spectroscopy (XPS) technology is extensively applied in the field of catalysts, offering deep insights into their electronic structures and chemical composition. The development of advanced techniques based on XPS instrumentation allows for a deeper and more holistic exploration of the characteristics of catalytic materials. This mini-review introduces and summarizes the primary applications of XPS-based analysis methods, including ion scattering spectroscopy (ISS) for analyzing single atomic layers, angle-resolved XPS, high energy X-ray sources and argon ion sputtering, each providing different depths of information about a sample. It also summarizes the use of inert atmosphere transfer devices and high-temperature reactors for quasi in situ monitoring as well as the integration of in situ techniques, including light irradiation XPS, to study catalysts' behavior under realistic conditions.

Keywords: catalyst; XPS; ion scattering spectroscopy; argon ion etching; in situ light irradiation

Citation: Cui, Y.; Liao, Y.; Sun, Y.; Wang, W.; Wu, J.; Dai, W.; Huang, T. Advanced XPS-Based Techniques in the Characterization of Catalytic Materials: A Mini-Review. *Catalysts* **2024**, *14*, 595. https://doi.org/10.3390/catal14090595

Academic Editor: Maurizio Muniz-Miranda

Received: 31 July 2024
Revised: 25 August 2024
Accepted: 25 August 2024
Published: 4 September 2024

1. Introduction

Surface characterization techniques are vital for the study of catalytic materials because catalytic reactions typically take place on the surface. Electron spectroscopy for chemical analysis (ESCA), well-known by the name of XPS [1,2], measures core-level binding energies (BEs) of ejected photoelectrons from atoms at or near a material's surface. The detection limit of the relative atomic proportion of surface elements (except H and He) is generally considered to be 0.1–1% [3–6]. The analysis depth of XPS is typically around 10 nm, which is not due to the limited penetration ability of X-rays, but rather due to the inelastic mean free path of emitted photoelectrons from the material's surface. Hence, XPS is widely employed in studying the electron transfer mechanism of heterogeneous catalysts. It can provide detailed insight into the elemental composition and chemical states of a surface, which are critical for understanding catalytic activity. XPS can also assess the stability and deactivation mechanisms of catalysts as well as study the interfaces and interactions of composite systems.

In recent years, the capabilities of XPS have been significantly enhanced by using various functional attachments that open up new avenues for research in the field of catalytic materials. For instance, the elemental distribution across the depth of a thin film (<10 nm) can be investigated through angle-dependent or angle-resolved XPS (ARXPS) by varying the take-off angle of the ejected electrons from the film surface. Utilizing a high-energy X-ray source (Ag Lα or Cr Kα) facilitates non-destructive depth profiling (<50 nm) [7,8]. Synchrotron radiation X-ray photoelectron spectroscopy allows for a broader range of non-destructive depth analysis by varying the energy of incident X-rays [9–12]. Coupled with argon ion etching techniques, this enables XPS analysis to penetrate to significantly deeper levels, even extending into the scale of micrometers [13,14]. Catalysts that react after high temperature pre-reduction or in a reducing atmosphere are very sensitive to air; therefore, special handling is required when they are transferred for XPS testing. Inert atmosphere transfer devices ensure that catalytic materials to

be tested do not make contact with air during the transfer process. A high-temperature catalytic reactor enables quasi in situ monitoring, which is crucial for understanding the mechanisms of catalytic reactions and the deactivation mechanisms of catalysts. In situ characterization methods could provide the actual reaction conditions by introducing a range of environmental variables, including elevated temperatures, exposure to light, and specific atmospheric conditions (near-ambient pressure XPS, NAPXPS), which allows real-time observation of the structure of catalysts and reaction products during the reaction process.

This mini-review focused on the applications of XPS functional accessories and in situ techniques in the characterization of catalytic materials. The applications of XPS functional accessories included ISS, high energy X-ray sources, and argon ion etching. Quasi in situ testing included the applications of inert atmosphere transfer devices and high-temperature catalytic reactors. We also reviewed the progress of in situ light irradiation XPS. The advantages, limitations and outlooks of these techniques were also discussed.

2. Conventional XPS Technology and Functional Accessories (Analysis at Different Depths)

The distinctive technical attributes of XPS render it a vital instrument for surface analysis, particularly within the realm of catalysis studies [15–18]. J. Y. Zhang et al. [19] used XPS to analyze the valence state of elements on the surface of prepared Ni-based electrocatalysts. By measuring the Ni 2p3/2 and Ni 2p1/2 peaks, it was determined that Ni on the sample surface exists in the form of Ni^{2+}, potentially forming a NiO surface layer. When combining XPS results with electrochemical tests and X-ray Absorption Spectroscopy (XAS) results, new insights into the structure of the active sites of the electrocatalysts were provided, especially the identification of low-coordinated Ni^{2+} centers (with pyramidal symmetry) and high-valence state Ni (Ni^{3+}) species, which facilitated the electrocatalytic oxygen evolution reaction. XPS was used by Wang's group to identify the oxidation states of Pt in the alloyed Pt single-atom catalysts [20]. The absence of Pt^0 peaks in the Pt 4f region confirmed the absence of Pt nanoparticles in the samples, which was consistent with observations from a high-resolution transmission electron microscopy (HR-TEM). The presence of both Pt^{2+} and Pt^{4+} species in the catalyst indicated an electron transfer interaction between Pt and its supporting substrate, ruthenium (Ru). The characterization of defect sites is crucial for the study of catalytic material activity. XPS plays a key role in characterizing defect sites. By analyzing the binding energy and intensity changes of photoelectron peaks, it can reveal the chemical status and electronic structure of a material's surface, plus identify and quantify surface defects such as oxygen vacancies, thereby gaining an in-depth understanding of the impact of these defects on the material's performance. Q. P. Huang et al. [21] used XPS analysis to demonstrate that the formation of oxygen vacancies can induce charge transfer from CeO_2 to Fe_2O_3 and redistribute the interfacial electron density, which contributes to enhancing the material's high-efficiency electrochemical water oxidation activity. XPS can also be used to analyze the structure and composition of Pt-Au bimetallic nanoparticles, as well as changes in the alloying process and the distribution of elements on a surface at different temperatures. This provides important information for understanding the surface catalytic activity and stability of bimetallic nanoparticles [22].

Expanding the functionality of an XPS instrument with related accessories enables it to perform testing and analysis at varied depths using various analysis methods, including from the monoatomic layer on the material's surface to depths approaching the scale of micrometers. These methods are presented in order of increasing depth, allowing them to probe different regions of a material from its outermost surface to its inner structure.

2.1. ISS (The Analysis Depth Is Less than 0.5 nm)

ISS, also named LEIS (Low-energy ion scattering spectroscopy), is a highly surface-sensitive technique that can detect the outermost atomic layer of a surface, providing information on the top monolayer of atoms [23–26]. Common ISS is equipped on an XPS instrument, with inert gas introduced into the argon ionization chamber for ionization.

The electron energy analyzer of XPS can measure the kinetic energies of surface-scattered ions by reversing the analyzer's polarity. In addition, there are also independent ISS instruments, such as HS-LEIS (high sensitivity-low energy ion scattering), which can be used in combination with ion etching to achieve higher-resolution depth profiling [27,28].

In the realm of heterogeneous catalysis, reactions take place at the outermost atomic layer of solid catalysts. Therefore, ISS is of crucial importance in the fundamental study of catalysis as well as in the optimization of industrial catalysts. R. Lang et al. [29] used ISS for studying the Pt migration on the surface of Fe_2O_3 during the calcination process. The Pt:Fe atomic ratio within the outermost surface layer decreased from 0.45 to 0.18 as the calcination temperature was increased from 773 K to1073 K while under flowing air (Figure 1), while the total Pt content determined by inductively coupled plasma spectrometry-atomic emission spectrometry (ICP-AES) remained unchanged. This indicated the migration of Pt atoms into the near sub-surface region of the Fe_2O_3 support.

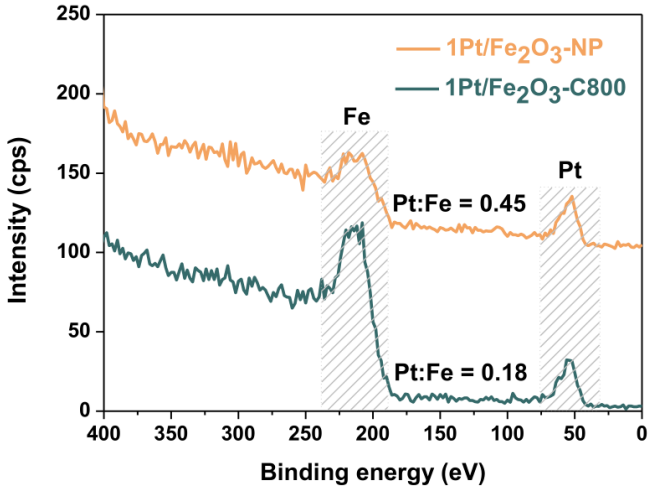

Figure 1. ISS data for 1Pt/Fe_2O_3-NP before and after calcination [29]. Copyright 2019 Nature Communication.

J. Hu et al. [30] used HS-LEIS for illustrating a more in-depth understanding of the synergistic effect among $CuZnAlO_x$ catalysts (Figure 2). For the Cu/Al_2O_3 catalysts, after H_2 reduction, the surface copper content showed a decreasing trend with an increase in reduction temperature. This could be due to the aggregation of copper particles at high temperatures leading to a reduction in the number of surface copper atoms. After sputtering (using Ne^+ as the ion source for sputtering), the ratio of Cu to Al intensity decreased, indicating that no additional overlayers were formed and the aggregation of copper was the main reason for the decrease in surface copper content. For the Cu/ZnO catalysts, similarly, the surface copper content significantly decreased with an increase in reduction temperature, suggesting more pronounced aggregation of copper particles or coverage by other substances. Yet, after sputtering, the ratio of Cu to Zn increased, indicating that during the sputtering process, the copper signal intensified while the zinc signal decreased. This phenomenon indicated that a ZnO_x overlayer may have formed on the surface that was gradually removed during sputtering, causing the copper signal to become more prominent. Combined with other characterizations, it was suggested that Cu^+, Cu^0, and the adjacent highly defective ZnO_x overlayer could work together to exert catalytic activity.

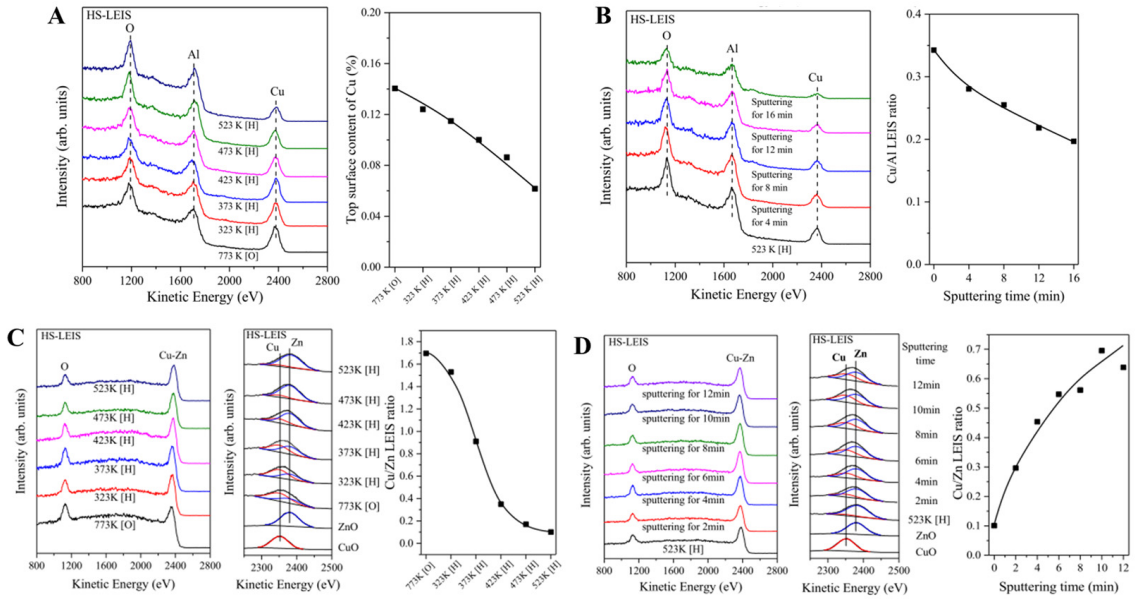

Figure 2. HS-LEIS data of 5 wt.%Cu/Al_2O_3 (**A**,**B**) and 5 wt.%Cu/ZnO (**C**,**D**) under different treatment conditions ([O]: oxidation, [H]: reduction, Sputtering: Ne^+ etching) [30]. Copyright 2021 Elsevier.

2.2. Angle-Resolved XPS (The Analysis Depth Is about 1~10 nm)

Angle-dependent XPS is a standard feature on many instruments that enables non-destructive surface analysis at different depths (at a maximum within 10 nm for Al Kα X-ray sources) of a sample by tilting the sample holder (Figure 3). Another method, ARXPS, obtains data at different depths by changing the photoelectron collection angle without tilting the sample holder (Figure 4). ARXPS is faster than traditional angle-dependent XPS measurements, and the analysis area remains the same and does not vary with the angle of electron emission. While ARXPS can provide more precise surface analysis, it often requires dedicated instrument configurations. ARXPS is highly sensitive to the chemical compositions, electronic states, and atomic arrangements at various depths, providing valuable insights into the properties of materials in a non-destructive manner. It is particularly useful for studying thin films, multilayers, and the effects of environmental processes on surfaces, making it a powerful tool for investigating enrichment effects and preferential orientation of molecules at the surface [31–33].

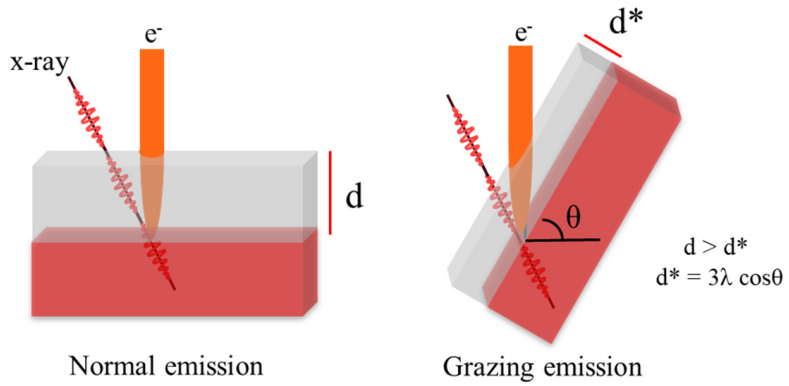

Figure 3. When the sample undergoes rotation with the X-ray source and detector remaining stationary, the effective depth decreased by a factor a factor of cos θ. λ represents the electron's inelastic mean free paths. d is the analysis depth at take-off angle of 90°; d* is the analysis depth at take off angle of (90° − θ).

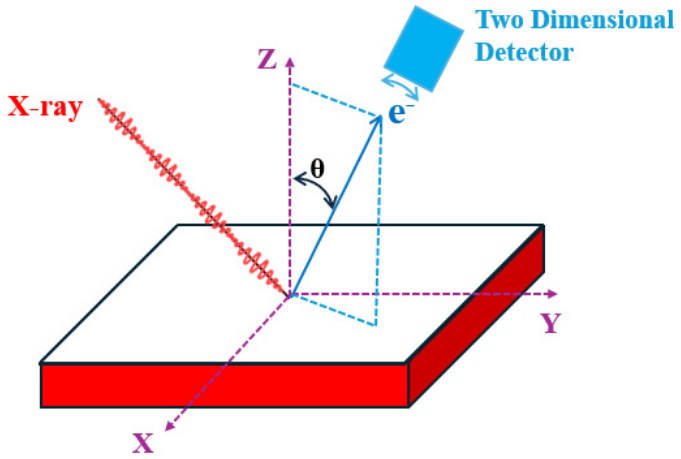

Figure 4. The X-ray source and sample holder remain stationary while a two-dimensional detector collects electrons at various angles.

Daniel Hemmeter et al. [34] used ARXPS for investigating the enrichment of platinum (Pt) complexes at the surface of ionic liquids (ILs) (Figure 5). By measuring the intensity of photoelectrons emitted at different angles, ARXPS could discern the concentration differences between the surface and the bulk, revealing the enrichment phenomenon of Pt complexes at the IL's surface. ARXPS assisted researchers in understanding how surface-active ligands influence the distribution of Pt complexes on ILs. Notably, fluorinated ligands exhibited surface activity that, akin to buoys, pulled the metal complexes toward the surface. When comparing the signal intensities for 0° and 80° emission angles, ARXPS unveiled the orientation of Pt complexes in the surface layer, with fluorinated side chains pointing towards the vacuum and the metal center positioned below. In summary, ARXPS was not only employed to analyze the surface enrichment and orientation of Pt complexes in ionic liquids, but it was also combined with surface tension measurements for providing in-depth insights into the design of catalyst systems.

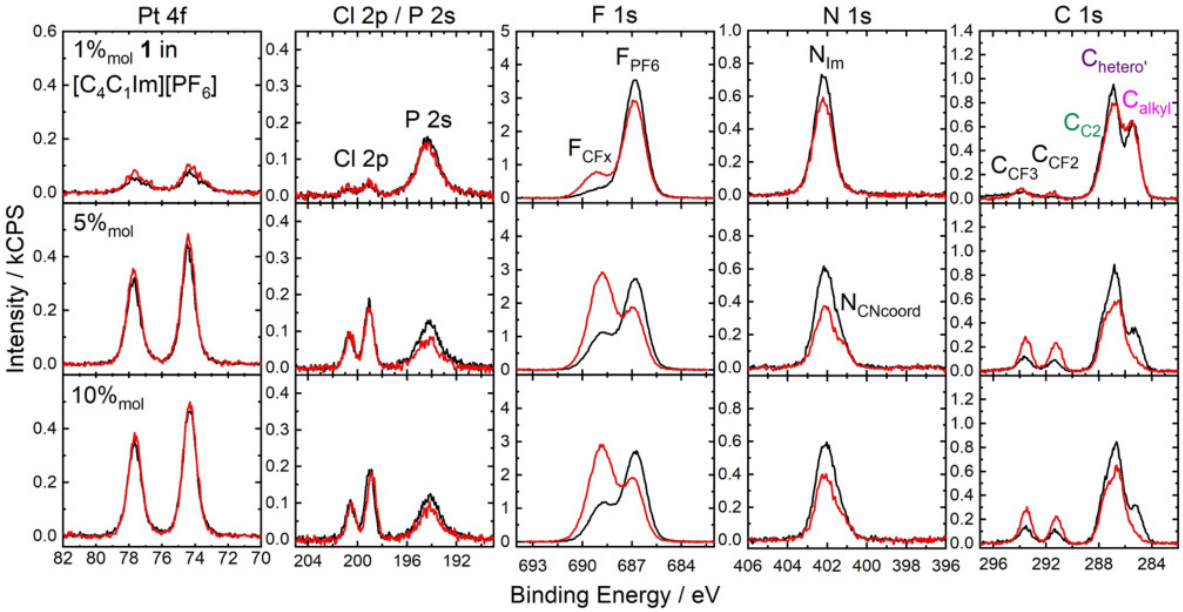

Figure 5. Pt 4f, Cl 2p/P 2s, F 1s, N 1s and C 1s spectrum of solutions of $[PtCl_2(C_3CNPFC_4Im)_2][PF_6]_2$ in $[C_4C_1Im][PF_6]$ with 1 $\%_{mol}$, 5 $\%_{mol}$ and 10 $\%_{mol}$ catalyst concentration in 0° (black) and 80° emission (red). All spectra were recorded at room temperature [34]. Copyright 2023 Wiley.

We collaborated with Ma's group to use ARXPS technology to characterize a catalyst structure that was designed for the electrocatalytic reduction of carbon dioxide [35]. A core-shell structure was created through the self-assembly of cetyltrimethylammonium bromide (CTAB) bilayers on the surface of gold nanorods (GNR). The CTAB bilayer acts as an analogue to a chloroplast membrane, facilitating the coordinated transport of carbon dioxide and protons. ARXPS was employed to confirm the presence of CTAB molecules on the GNR surface, and depth-resolved analysis was conducted to further investigate the molecular arrangement of the surface-modified CTAB molecules. The N 1s peak observed at a shallow analysis depth indicated that the polar headgroups of the CTAB molecules were oriented towards the exterior of the GNR surface. The emergence of additional nitrogen species at higher probing depths confirmed the formation of a bilayer structure of CTAB molecules on the GNR surface.

2.3. High Energy X-ray Source (X-ray Sources Involved in This Article Have an Analysis Depth of Less than 50 nm)

Currently, common XPS equipment typically uses a fixed-energy X-ray source (Al Kα, 1486.7 eV). Utilizing synchrotron radiation as the light source for XPS provides a broader range of X-ray energies, enabling synchrotron radiation XPS (SRXPS), also known as hard X-ray photoelectron spectroscopy (HAXPES), in order to achieve higher energy resolution and/or deeper analysis depth. However, synchrotron radiation beam sources are currently not very abundant. In recent years, the capacity to measure XPS data with both Al Kα and high-energy X-ray sources on a single device enhances its analytical capabilities. Conventional dual-anode instruments benefit from the Mg Kα source (1253.6 eV) to mitigate interference from Auger electrons that occur for Al Kα. However, the modest energy gap of around 230 eV between the two sources means that some significant elements and alloys can still exhibit auger electron interferences for both. Besides, non-monochromatic dual anodes typically offer lower resolution and may necessitate the analysis of X-ray satellites for data interpretation. In contrast, a high-energy X-ray source like Ag Lα (2984.3 eV) presents a substantial energy difference of about 1500 eV from the Al Kα and is also monochromatic. This feature simplifies the differentiation of Auger electron interferences, particularly for 3d transition metals where the LMM Auger peaks overlap critical regions when using either Al Kα or Mg Kα X-rays. We used monochromatic Al Kα, monochromatic Ag Lα, and non-monochromatic Mg Kα as X-ray sources for GaN analysis (Figure 6). Different separations of Ga LMM and N 1s spectra results were obtained with three anode materials. The Ga LMM was overlapped with N 1s on Mg and Al anodes, while it was completely separated on Ag anodes, leading to the easy analysis of N 1s [36]. Furthermore, for the interference between spectral peaks of different elemental orbitals, such as Ni 3p and Al 2p, the binding energy does not change with the alteration of the X-ray source. Employing a high-energy X-ray source can yield information from inner orbitals, like Al 1s. This enables the analysis of aluminum's chemical state (Figure 7). An additional application lies in determining the depth profile of elements [7]. The Ag Lα source offers deeper probing capabilities, but it has an intensity approximately 50 times less than the Al Kα source, which limits its application to a certain extent. In addition, other commonly used high-energy X-ray sources such as Cr Kα (5414.7 eV) can further improve the analysis depth of XPS, which is particularly useful for analyzing multi-layer thin films or samples with complex structures [37–39].

Mark A. Isaacs et al. [8] acquired the Mg 2p spectrum utilizing monochromated Al Kα and Ag Lα excitation sources. They employed inelastic mean free paths of 4.6 nm and 8.1 nm, respectively, to evaluate the vertical distribution of magnesium. The Mg to Si atomic ratio was determined to be 0.05 for the Ag Lα source and 0.008 for the Al Kα source. These findings confirmed that magnesium was located deep within the SZ/MgO/MM-SBA-15 framework, consistent with the expected mesopore localization.

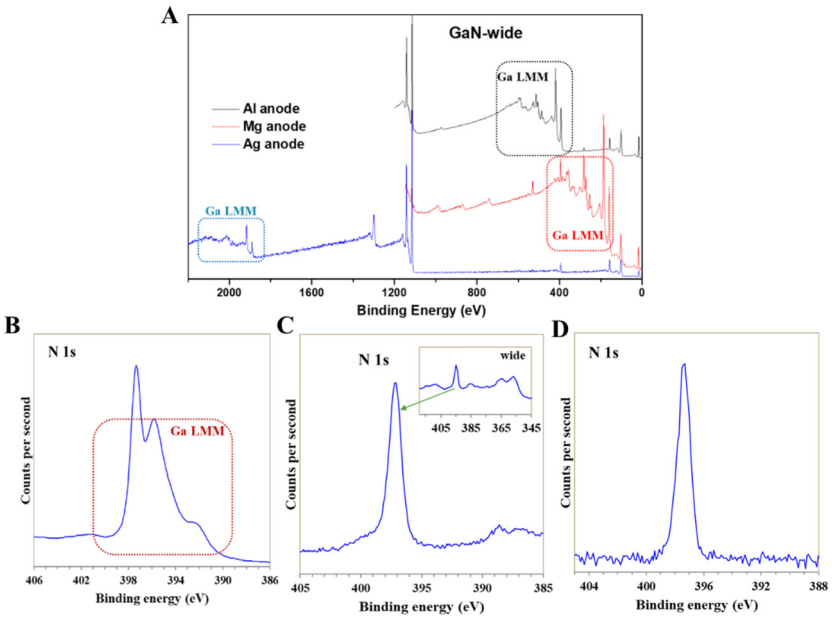

Figure 6. Wide spectrums of GaN with different anodes (**A**) N 1s spectrum of GaN with Al anode (**B**), Mg anode (**C**) and Ag anode (**D**) [36]. Copyright 2023 Journal of Fudan University: Natural Science.

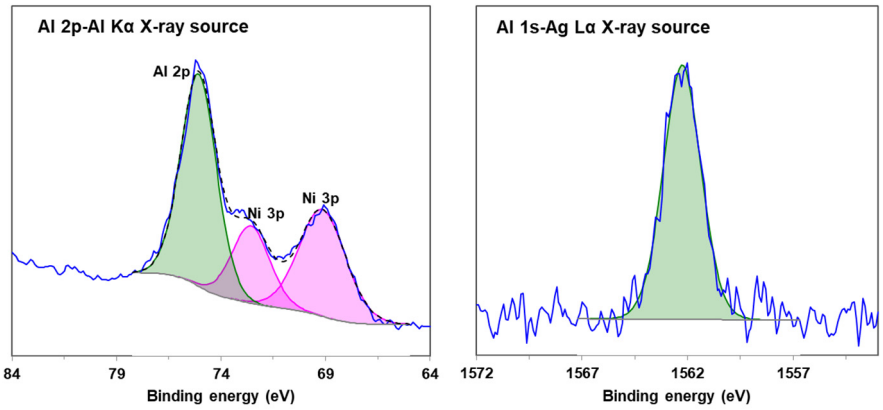

Figure 7. Al 2p spectrum collected using Al Kα source (**left**) and the Al 1s spectrum collected using Ag Lα source (**right**).

2.4. Mono Argon Ion and Argon Cluster Ion Etching (The Analysis Depth Is about 10 nm~2 µm)

Argon ion beam techniques allow researchers to delve into the surface and subsurface regions of catalytic materials to obtain comprehensive information about their chemical composition and state [40]. The application of argon etching technology in the characterization of catalytic materials generally involves surface cleaning, to remove surface organic contaminants, and depth analysis, to characterize the distribution of elements along depth or the characterization of core-like shell structures composed of different elements [14]. Recently, sputtering by cluster Ar ions has become of scientific and technical interest compared with mono Ar ions because of how the former causes less chemical and electronic damage to a sample's surface. Various dimensions of Ar clusters can be formed by the adiabatic expansion of Ar gas in a nozzle as it passes from a high-pressure side to a vacuum chamber [41–43], where it is then ionized, separated, and accelerated. The energy per Ar atom would be very low for large number clusters, such as 10 keVAr_{1000}^{+} mode, whose energy per Ar atom is about ~10 eV. The low-energy cluster mode is generally used for the removal of surface organic contamination or the in-depth analysis of organic films, while the high-energy cluster mode (20 keVAr_{500}^{+}) can provide an in-depth analysis of inorganic materials [44,45].

We cooperated with Q. Hua et al. [46] to illustrate the valence states and depth distribution of Sn in $C_{12}A_7$:e^- nanoparticles using XPS combined with argon ion etching technology. It was observed that the Ca/Al ratio remained constant regardless of the sputtering depth, whereas the ratios of Sn/Al and Sn/Ca exhibited a decline with a higher surface concentration (Figure 8A,B), which indicated that the distribution of Sn within the Sn-doped $C_{12}A_7$:e^- nanoparticles is not uniform. We also compared the valence states and depth distribution of Sn in the $C_{12}A_7$:e^- nanoparticles during the Ar^+ ion (1 keV) and Ar cluster ion (10 keV Ar_{1000}^+) sputtering process. Figure 8C,D show that both Ar^+ ions and Ar cluster ions result in the reduction of surface Sn^{4+} (~487.5 eV). However, the binding energy and the relative proportion of Sn^{4+} for Ar^+ ion etching were lower than those for Ar cluster ion sputtering, indicating that the reduction of Sn^{4+} under the Ar^+ ion etching mode was more severe.

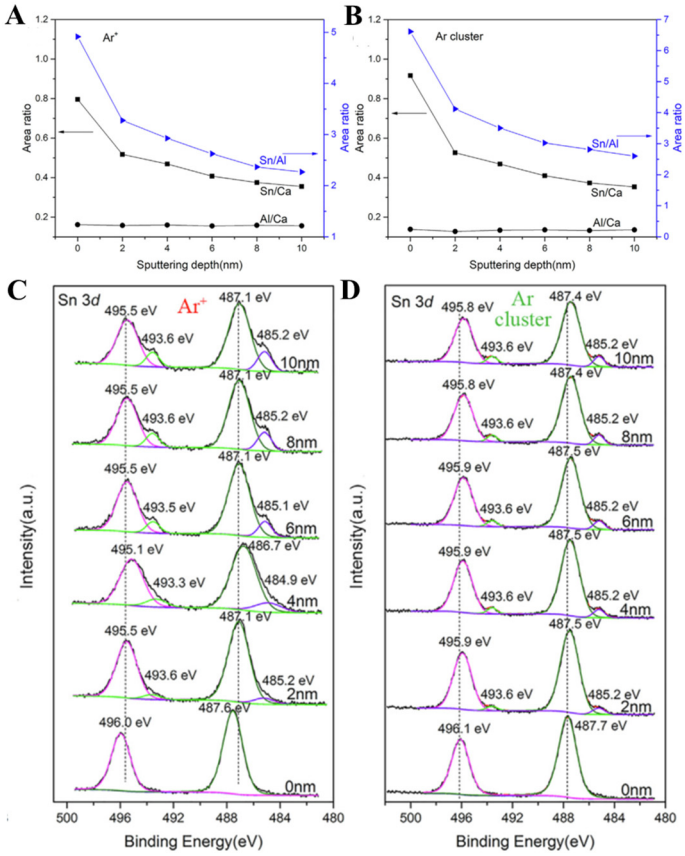

Figure 8. The change of the atomic ratio of Sn, Al, Ca as a function of sputtering depths and Sn 3d as a function of sputtering depths under Ar^+ (**A**,**C**) and Ar cluster etching (**B**,**D**) [46]. Copyright 2020 Elsevier.

We cooperated with L. Zhang et al. [47] to employ argon cluster sputtering to characterize sub-surface elemental and chemical state information. In the case of the composite sample 10% NiS/m-CN-160-12, XPS results indicated the surface was covered by amorphous $Ni(OH)_2$ layers that obscured the underlying NiS species from the XPS analysis. After sputtering by a 10 keVAr_{1000}^+ argon cluster, the surface layers were removed, allowing the detection of NiS species that were not initially accessible.

In order to explore the interfacial interaction of TpBpy/20%$NaTaO_3$ composites (TpBpy, constructed from triformylphloroglucinol (Tp) and 2,2′-bipyridine (Bpy)), we worked with Dai's group [48] using argon clusters to remove a surface organic TpBpy layer. The XPS signal of Ta 4f within the composite became more intense with increasing etching time. Furthermore, the binding energies of Ta 4f in the TpBpy/20%$NaTaO_3$ composite negatively shifted compared to those of pure $NaTaO_3$ during the argon ion etching process,

suggesting an increased electron density around $NaTaO_3$ within the heterostructure. This finding, along with in situ XPS and density functional theory (DFT) calculation results, demonstrated the transfer of photogenerated electrons from $NaTaO_3$ to TpBpy, implying the formation of an S-scheme heterostructure between TpBpy and $NaTaO_3$.

3. Quasi In Situ XPS

XPS has been established as one of the best analytical techniques to probe the composition and electronic structures of catalysts [49]. Nevertheless, the drying process and exposure to air during the transfer between chambers can lead to contamination and the introduction of unwanted functional groups on the surface of the catalyst. This interference can obscure the spectroscopic signals that reveal the characteristics of the active sites [50,51]. Especially for air-sensitive catalysts, particularly after high-temperature reduction or post-reaction, it is necessary to transfer the sample into the spectrometer under inert atmosphere protection, or to perform the reaction directly in the instrument's built-in reaction chamber and then immediately transfer it to the analysis chamber for testing. However, it is worth noting that traditional XPS spectrometers operate under ultra-high vacuum (UHV) conditions, which pose significant limitations in real time monitoring under actual reaction conditions [52]. Recently developed XPS spectrometers capable of operating in the mbar pressure range allow for the study of the catalyst's surface under reaction conditions, facilitating the in situ real-time description of the interactions between the catalyst and the gases or vapors involved in the reaction [53]. However, there is still a difference between the chamber pressure and the actual reaction pressure. This review will concentrate on methodologies that enable the utilization of conventional laboratory XPS instruments to investigate air-sensitive catalysts and to conduct experiments in a quasi in situ fashion.

3.1. Transfer of Samples under Inert Atmosphere

An inert transfer device facilitates the loading of air-sensitive samples within a glovebox. After loading, a sealed valve is closed to ensure that the samples are preserved under either a vacuum or an inert gas environment. The samples are subsequently transferred from the glovebox to the analytical instrument. A flange is directly attached to the pre-vacuum chamber of an XPS instrument (Figure 9, left). When the pressure inside the pre-vacuum chamber matches the desired level, the gate valve is opened to allow the transfer of the samples into the main chamber of the instrument for further analysis [54]. If the sample chamber is directly connected to the glove box directly, samples can be loaded and transferred within the glove box (Figure 9, right).

Figure 9. A sample transfer under vacuum or inert gas (**left**) from Kratos Analytical and a glovebox (**right**) connected to the instrument's pre-pumping chamber.

The valence state of Ir affected the selectivity of the CO_2 hydrogenation reaction. In D. Ma's work [55], XPS was employed to examine the oxidation state of iridium in the 20Ir/Ce-OH samples extracted at various time intervals during the synthesis process. The Ir 4f XPS spectra in Figure 10A revealed that only Ir^{3+} species were resolved throughout the entire synthesis process, indicating that the iridium species were not reduced during

the preparation. The surface chemistries of the Ir/Ce catalysts after the CO_2 hydrogenation reaction (referred to as Ir/Ce-used catalysts, see Figure 10B) were also evaluated. For the catalyst with 20 wt.% iridium loading, a symmetric peak in the Ir 4f XPS spectrum was attributed to metallic iridium. When the iridium loading was decreased to 15%, the Ir 4f peak broadened and shifted to a higher energy, suggesting that the iridium species were partially positively charged. A further reduction in iridium loading to 5 wt.% showed a 0.5 eV shift in the Ir 4f peak position compared to the 20 wt.% loaded catalyst, confirming partial oxidation of the iridium species. All catalysts involved in this work were transferred by inert gas transfer.

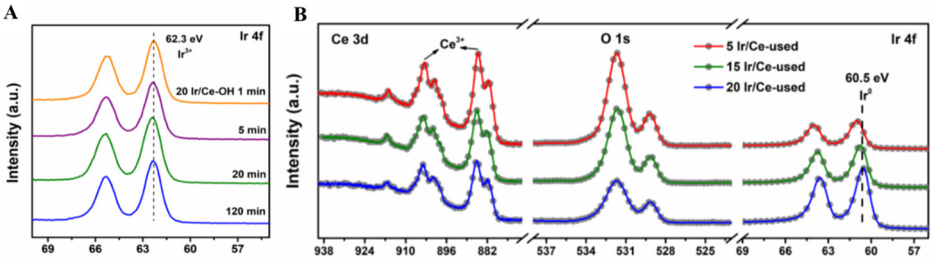

Figure 10. Ir 4f XPS spectrums of the 20 Ir/Ce-OH nanohybrids taken out of the synthetic mixture at different time intervals (**A**) and the Ce 3d, O 1s, Ir 4f spectra of the Ir/Ce-used catalysts (**B**) [55]. Copyright 2017 Wiley.

G. C. Zhang et al. [56] used XPS to investigate the surface electronic structures of copper (Cu), indium (In), and oxygen (O) species in Cu-based catalysts. The catalyst was transferred into the XPS transfer chamber within a vacuum glove box. The amount of Cu^+ and oxygen vacancies is correlated with the catalytic performance.

3.2. High Temperature Cat Cell

Inert transfer techniques facilitate the possibility of conducting quasi in situ XPS tests. However, the process traditionally involves sample collection and transfer, which may lead to surface alterations because of exposure to air or other environmental factors. To circumvent this issue and enable more flexible investigation of the catalyst's surface elemental information under various reaction conditions, a high-temperature gas catalytic reaction chamber is introduced (See Figure 11). H_2, CO, CO_2, CH_4, and other non-corrosive gases can be introduced into the chamber and subjected to reactions at specific temperatures. This advancement allows catalysts to be directly transferred to the analysis chamber for testing without the need for intermediate handling, thus minimizing the risk of surface changes [57–59].

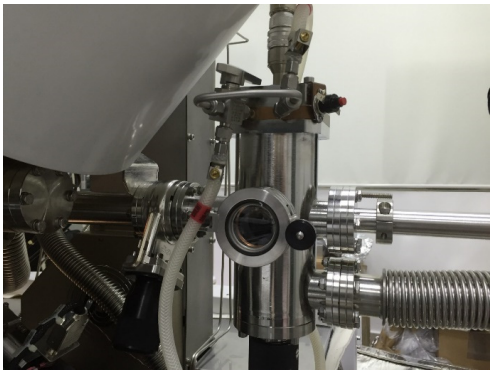

Figure 11. High temperature cat cell from Kratos Analytical.

Cu-based catalysts are widely used in many important chemical reaction processes, including syngas conversion, CO/hydrocarbon selective oxidation, methanol steam re-

forming, and alcohol dehydrogenation, etc. W. B. Fan's group [60] designed and prepared a Cu/SiO_2 core-shell structure catalyst with an extremely high stability using the typical C1 reaction of methanol dehydrogenation to prepare methyl formate as the model reaction. A high-temperature gas reaction cell system was used to study the catalyst under different reaction temperatures, reaction times and loadings (Figure 12). The relationship between the catalyst surface, the active species, and the product in the catalytic reaction was systematically revealed, and it was possible to deeply understand the reaction induction period, catalytic mechanism and reaction path. XPS analysis revealed the state of copper species on the surface after reduction at different temperatures. Quasi in situ XPS monitored the changes in copper species on the catalyst surface during the reaction process, such as the rapid oxidation of Cu^0 to Cu^+ and the subsequent gradual reduction back to Cu^0 during the methanol dehydrogenation (MDM) reaction; the regeneration capability of the catalyst could also be evaluated.

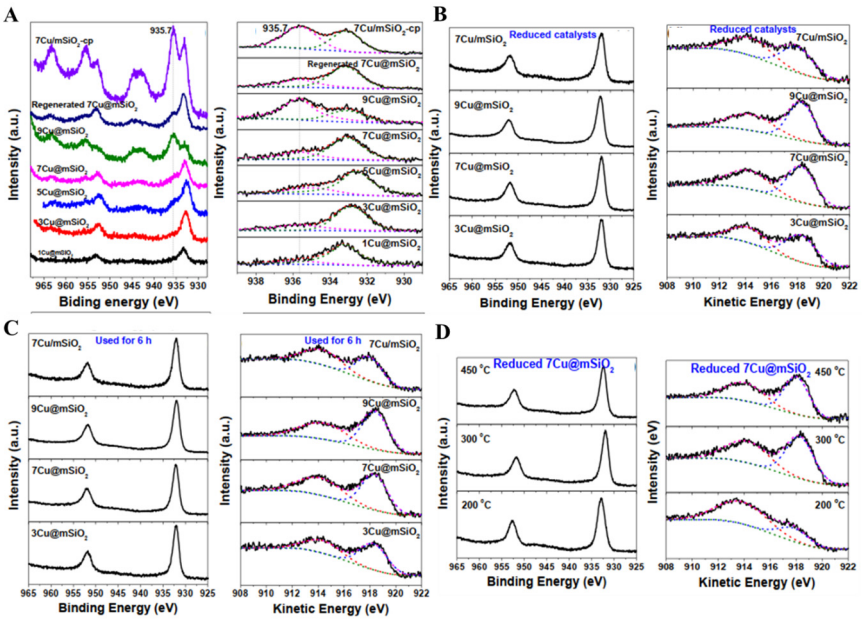

Figure 12. XPS spectra of Cu-based catalysts. (**A**) Cu 2p and Cu 2p3/2 XPS spectra of calcined $xCu@mSiO_2$, regenerated $7Cu@mSiO_2$ and copper phyllosilicate ($7Cu/mSiO_2$-cp); (**B**) in situ Cu 2p XPS and Cu LMM spectra of Cu-based catalysts reduced at 573 K; (**C**) in situ Cu 2p XPS and Cu LMM XAES spectra of Cu-based catalysts after reaction of 6 h; (**D**) in situ Cu 2p XPS and Cu LMM spectra of $7Cu@mSiO_2$ reduced at different temperatures [60]. Copyright 2018 Wiley.

A high-catalytic activity and high-stability catalyst Ni/CeO_2 for C-O hydrogen hydrolysis of biomass-derived furanic compounds was prepared by F. W. Li's group [61]. The structural characteristics of Ni species in the xNi/CeO_2 catalyst and the evolution of Ni species during preparation were analyzed by a quasi in situ XPS technique. By analyzing the correlation between XPS results and catalytic activity data, the roles of surface Ni^0 and $Ni^{\delta+}$ species in C=C hydrogenation and C-O hydrogenolysis were identified, with Ni^0 inferred as the active center for C=C hydrogenation and $Ni^{\delta+}$ for C-O hydrogenolysis. By changing the Ni load to optimize the relative contents of Ni^0 and $Ni^{\delta+}$, the kinetics matching of C=C hydrogenation and C-O hydrolysis reaction rates was achieved, and the best catalytic performance was obtained.

Furthermore, the latest technological advancements now permit the introduction of light sources within the aforementioned high-temperature gas reaction chambers of XPS instruments. This capability enables the study of catalytic reactions under in situ light irradiation followed by quasi in situ XPS analysis (Figure 13).

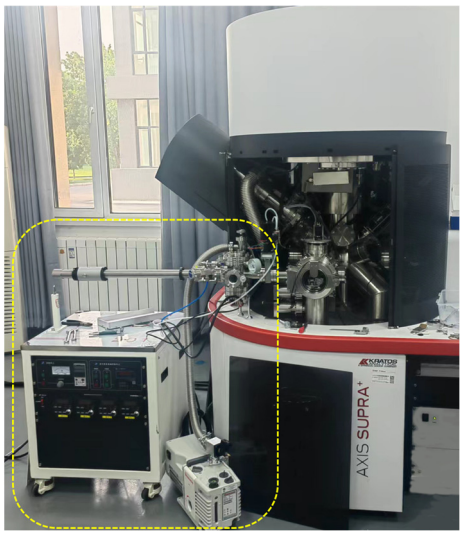

Figure 13. A high temperature cat cell capable of in situ irradiation connected to the instrument's pre-pumping chamber.

4. In Situ Irradiated XPS (ISI-XPS)

Conventional XPS can gain accurate information about the chemical state of atoms and the electron transfer between composites. ISI-XPS is an advanced analytical technique that has been increasingly utilized in the study of photocatalytic materials. This technique allows for the direct observation of electron transfer and interfacial bonding under light excitation (simulating real reaction conditions), providing real-time information on the dynamics of photogenerated charges within a photocatalytic system [62–64]. ISI-XPS can capture changes in the valence band maximum due to light exposure, allowing for the determination of key parameters such as the bandgap and band bending. By analyzing the chemical state of dopants under light exposure, this technique can identify the type of doping in semiconductors [65,66]. Additionally, variations in binding energy at peak positions under different light exposure conditions can be used to study charge transfer dynamics and monitor changes in the surface potential of photoresistors [67]. Employing a short-pulse laser as the excitation source and XPS as the probe enables the investigation of ultrafast electron processes within the material, such as electron excitation, thermalization, and relaxation [68]. UPS is often used in conjunction with this technique in order to characterize the band structure of materials. P. Zhang's group [69] published a review on the development of ISI-XPS in electrospinning photocatalysis, and K. L. Huang's group [70] has also contributed an extensive review article to the field of in situ characterization techniques, including ISI-XPS, as applied in photocatalysis. These two reviews cover some of the typical studies that involved in situ illumination XPS prior to 2022, but do not contain many experimental details. ISI-XPS is operated based on traditional XPS spectroscopy by introducing an ultraviolet and visible light source. Generally, there are two ways to introduce light: one is to irradiate through the observation window during the test, and the other is to introduce optical fibers into the vacuum chamber through a flange and connect to an external light source (see Figure 14). In consideration of X-ray radiation, the observation window of an XPS instrument is typically constructed with two layers of glass. The inner layer is made of quartz glass, while the outer layer is made of lead glass. Both glass types have a certain absorption of light in different ultraviolet wavelengths, so when irradiating through the observation window, one should pay attention to the selection of irradiation wavelength, or the operator can also remove the lead glass directly.

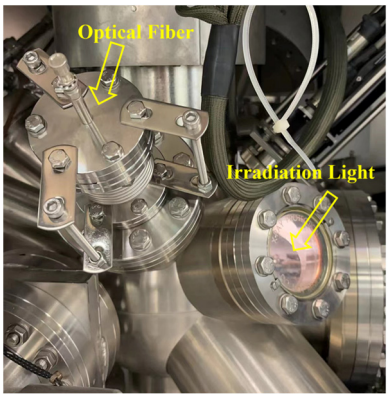

Figure 14. External light exposure and fiber optic introduction from Kratos Analytical.

We cooperated with H. J. Gu et al. [71] to utilize ISI-XPS (ultraviolet wavelength light) to verify the surface charge transfer process between CdSe and MXene. While the binding energy of Cd 3d and Se 3d peaks shifted positively under light irradiation, the binding energy of Ti 2p peaks shifted negatively, suggesting the transfer of electrons from CdSe to MXene (Figure 15).

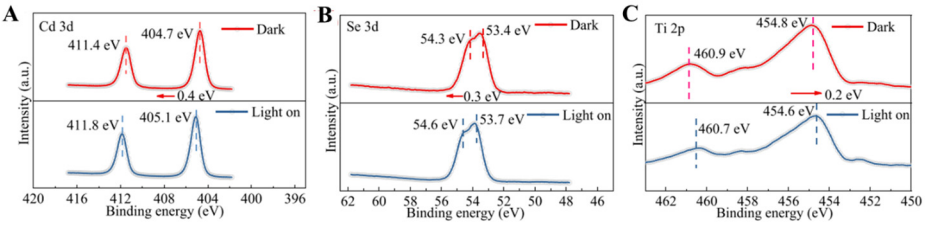

Figure 15. High-resolution in situ XPS spectra of Cd 3d (**A**), Se 3d (**B**), and Ti 2p (**C**) of CdSe-MXene [71]. Copyright 2023 Elsevier.

We cooperated with W. Luo and Q. Xiao's group [72] to demonstrate the application of ISI-XPS in investigating the surface chemical states and electronic properties of ruthenium (Ru) cocatalysts supported on Ga-doped $La_5Ti_2Cu_{0.9}Ag_{0.1}O_7S_5$ (LTCA) photocatalysts. The ISI-XPS measurements were conducted under visible light irradiation conditions in order to monitor the changes in the Ru 3d XPS spectra of the Ru (CN = 3.4) AC/LTCA sample at different time intervals. A significant finding was that the binding energy of the Ru 3d5/2 core levels exhibited a negative shift with increasing irradiation time, indicating a decrease in the oxidation state of Ru. After 20 min of irradiation, an approximate shift of −0.18 eV was observed, which suggested that the photocatalyst LTCA, acting as the light absorber, generated a substantial number of electrons under irradiation. These photogenerated electrons were then transferred to the surface Ru atomic clusters, which became enriched with electrons and enhanced the photocatalytic H_2 production activity. Experiments that involve altering the wavelength of irradiation light are crucial for understanding the photoelectron transfer process at the semiconductor interface. Y. M. Huang et al. [73] discovered that photogenerated electrons were transferred from COF-TpBpy (a covalent organic framework assembled with bipyridine linkages) to VNbC (VNbC solid-solution MXene heterostructures) using ISI-XPS, thereby enhancing electron transfer efficiency in the entire photocatalytic process.

P. Zhang's group [74] investigated how different light energies affect the behavior of photogenerated electrons within heterojunction catalysts by systematically changing the wavelength from the visible to the ultraviolet range (700 to 350 nm). The study revealed the dynamics of photogenerated electron transfer at the heterogeneous interface, demonstrating how the transfer process was influenced by the wavelength of the incident light. Their recent work has conducted a quantitative analysis of the number of photogenerated electron transfers in heterojunctions using variable wavelength in-situ irradiation [75].

5. Conclusions and Prospective

In conclusion, the integration of advanced XPS techniques has not only revolutionized the characterization of catalytic materials, but has also provided a multi-dimensional perspective on their behavior under various conditions. The ability to probe the surface and subsurface regions with high precision, combined with the capability to monitor reactions in real-time, has significantly deepened our understanding of catalytic processes. The application of ISS has shed light on the dynamics occurring at the atomic level, which is pivotal for the design of efficient catalysts. High-energy X-ray sources can reduce certain interferences from Auger peaks and elicit information from more inwardly located electron orbitals. Argon ion etching has further bridged the gap between surface analysis and bulk properties, offering insights into the distribution and state of elements within the material's depth. ISI-XPS has been a revolution, particularly in the field of photocatalysis, where understanding the behavior of materials under light irradiation is crucial. It has allowed researchers to directly observe the migration of photogenerated charges and the formation of intermediates, which are often elusive under ex situ conditions. The development of quasi in situ XPS methodologies has addressed a critical need in catalysis research: minimizing the impact of air exposure during sample transfer.

In response to the XPS instrument-related techniques mentioned above, we offer the following suggestions. Additionally, we have also provided an outlook on the related advanced techniques that are expected to be widely used in the characterization of catalytic materials in the future.

5.1. Improve the Quality of XPS Data Analysis

The power of XPS techniques and the accessibility of sophisticated commercial instruments make XPS a favored tool among researchers. First, it is essential to ensure the correctness of the test results. Peak splitting can occur due to differential charging, where the signal from an element is in the same chemical state while two distinct areas have varying local conductivity [76]. Secondly, it is important to ensure that XPS data is analyzed correctly. A recent survey of several high-quality journals indicated that approximately 40% of the XPS peak fits presented are entirely inaccurate, with an additional 40% being questionable [77]. For example, the areas of peaks do not follow 2:3 areas ratios for the spin-orbit splitting of the 3d signal [78]. Furthermore, the overlap interference between different elemental peaks, such as the overlap between auger peaks and orbital peaks, or the overlap of different orbital peaks, sometimes can be mistakenly attributed to new chemical species.

5.2. Further Study the Shift and Intensity Change of Spectra Peak in ISI-XPS Experiments

For semiconductors, exposure to ultraviolet or visible light can excite electrons to transition from the valence band to the conduction band. This excitation and the subsequent movement of charge carriers lead to alterations in the electron density surrounding the atoms in the excited state, which in turn affects the BE of the inner electrons. Once the illumination ceases, the photogenerated electrons should revert to the valence band and recombine with the holes, restoring the initial BE of the constituent atoms to their original states. Most of the reported work to date has focused on comparing the changes before and after light exposure, with little mention of the comparison between the peak positions after light exposure and their initial positions. In practice, our experiments revealed that the initial BE could not fully revert after turning off the light, which may be attributed to the thermal effect or surface reconstruction under light, and needs to be further studied. Additionally, influenced by the density of the outer electrons, there will also be some differences in peak intensity before and after light exposure, which should also be of concern to researchers.

5.3. The Measurement of Electrical Band Gap

In the photocatalysis field, the energy band structure of the semiconductors is important for mechanism studies. XPS and UPS are typically used to measure the position of the valence band maximum. The Tauc plot technique is a common approach for estimating band gaps, yet its accuracy can be inconsistent, particularly when differentiating between direct and indirect band gaps. For a more thorough and precise analysis, supplementary experimental methods such as XPS, UPS, and Inverse Photoelectron Spectroscopy (IPES) are recommended. However, these methods may not always be readily available [79]. This difference is due to the excitonic effects and the Coulomb interaction between the photogenerated electron-hole pair, which are not accounted for in the initial state measurements by XPS, UPS, and IPES. Therefore, further development of IPES techniques is required for more conclusive mechanistic studies.

5.4. Further Optimizing In Situ XPS to Deepen the Study of Catalytic Reaction Mechanisms

Because of electrons' limited IMFP, XPS has traditionally been confined to high-vacuum conditions, which minimize the interaction between photoelectrons and gas molecules, thereby reducing signal loss [80]. D. Weingarth et al. [81] applied ultra-high vacuum XPS tools for in situ investigations of electrochemical systems in ionic liquids as electrolytes. With the development of differential pumping systems in the early 2000s, ambient pressure XPS (APXPS) and near-ambient pressure XPS (NAP-XPS) gradually came into view for in situ/operando studies of catalytic systems, such as gas-solid phase catalysis and electrocatalysis [82]. However, the insights gleaned from such in situ or operando methodologies might not always align perfectly with the true conditions of the reaction, primarily due to inherent limitations in the cell's construction. This discrepancy could lead to a partial and potentially misleading understanding of the catalytic process. Furthermore, reaction intermediates and surface species on catalysts change dynamically over time, so in situ XPS technologies still suffer from lower sensitivity and spatiotemporal resolution. Therefore, we believe that enhancing instrument sensitivity (reducing the time for each scan), optimizing rapid scanning modes for testing, and decreasing the analysis spot size to capture changes in smaller areas could be potential directions for future development.

Author Contributions: Y.C. and Y.L. conducted the information search and wrote the first draft of the manuscript, Y.S., W.W., J.W., W.D. and T.H. discussed and revised parts of the manuscript. All authors have read and agreed to the published version of the manuscript.

Funding: This research was funded by the Natural Science Foundation of Shanghai (22ZR1404200).

Conflicts of Interest: Author Yuanyuan Cui, Youbao Sun, Wenchang Wang, Jinqi Wu and Taohong Huang were employed by the company Shimadzu China Co., Ltd. The remaining authors declare that the research was conducted in the absence of any commercial or financial relationships that could be construed as a potential conflict of interest.

References

1. Siegbahn, K. Electron spectroscopy for atoms, molecules, and condensed matter. *Rev. Mod. Phys.* **1982**, *54*, 709. [CrossRef]
2. Penn, D.R. Quantitative chemical analysis by ESCA. *J. Electron Spectrosc. Relat. Phenom.* **1976**, *9*, 29–40. [CrossRef]
3. Jain, V.; Biesinger, M.C.; Linford, M.R. The Gaussian-Lorentzian Sum, Product, and Convolution (Voigt) functions in the context of peak fitting X-ray photoelectron spectroscopy (XPS) narrow scans. *Appl. Surf. Sci.* **2018**, *447*, 548–553. [CrossRef]
4. Lubenchenko, A.V.; Batrakov, A.A.; Pavolotsky, A.B.; Lubenchenko, O.I.; Ivanov, D.A. XPS study of multilayer multicomponent films. *Appl. Surf. Sci.* **2018**, *427*, 711–721. [CrossRef]
5. Metson, J.B.; Hyland, M.M.; Gillespie, A.; Hemmingsen-Jensen, M. X-ray photoelectron spectroscopy applications to corrosion and adhesion at metal oxide surfaces. *Colloids Surf. A Physicochem. Eng. Asp.* **1994**, *93*, 173–180. [CrossRef]
6. Greczynski, G.; Hultman, L. X-ray photoelectron spectroscopy: Towards reliable binding energy referencing. *Prog. Mater. Sci.* **2020**, *107*, 100591. [CrossRef]
7. Shard, A.G.; Counsell, J.D.P.; Cant, D.J.H.; Smith, E.F.; Navabpour, P.; Zhang, X.; Blomfield, C.J. Intensity calibration and sensitivity factors for XPS instruments with monochromatic Ag Lα and Al Kα sources. *Surf. Interface Anal.* **2019**, *51*, 763–773. [CrossRef]

8. Isaacs, M.A.; Parlett, C.M.A.; Robinson, N.; Durndell, L.J.; Manayil, J.C.; Beaumont, S.K.; Jiang, S.; Hondow, N.S.; Lamb, A.C.; Jampaiah, D.; et al. A spatially orthogonal hierarchically porous acid–base catalyst for cascade and antagonistic reactions. *Nat. Catal.* **2020**, *3*, 921–931. [CrossRef]
9. Bukhtiyarov, A.V.; Prosvirin, I.P.; Saraev, A.A.; Klyushin, A.Y.; Knop-Gericke, A.; Bukhtiyarov, V.I. In situ formation of the active sites in Pd–Au bimetallic nanocatalysts for CO oxidation: NAP (near ambient pressure) XPS and MS study. *Faraday Discuss.* **2018**, *208*, 255–268. [CrossRef]
10. Alayoglu, S.; Somorjai, G.A. Ambient Pressure X-ray Photoelectron Spectroscopy for Probing Monometallic, Bimetallic and Oxide-Metal Catalysts Under Reactive Atmospheres and Catalytic Reaction Conditions. *Top. Catal.* **2015**, *59*, 420–438. [CrossRef]
11. Bukhtiyarov, A.V.; Prosvirin, I.P.; Bukhtiyarov, V.I. XPS/STM study of model bimetallic Pd–Au/HOPG catalysts. *Appl. Surf. Sci.* **2016**, *367*, 214–221. [CrossRef]
12. Languille, M.A.; Ehret, E.; Lee, H.C.; Jeong, C.K.; Toyoshima, R.; Kondoh, H.; Mase, K.; Jugnet, Y.; Bertolini, J.C.; Aires, F.J.C.S.; et al. In-situ surface analysis of AuPd(110) under elevated pressure of CO. *Catal. Today* **2016**, *260*, 39–45. [CrossRef]
13. Erickson, N.C.; Raman, S.N.; Hammond, J.S.; Holmes, R.J. Depth profiling organic light-emitting devices by gas-cluster ion beam sputtering and X-ray photoelectron spectroscopy. *Org. Electron.* **2014**, *15*, 2988–2992. [CrossRef]
14. Zemek, J.; Jiricek, P.; Houdkova, J.; Jurek, K.; Gedeon, O. Lead-silicate glass surface sputtered by an argon cluster ion beam investigated by XPS. *J. Non-Cryst. Solids* **2017**, *469*, 1–6. [CrossRef]
15. Krishna, D.N.G.; Philip, J. Review on surface-characterization applications of X-ray photoelectron spectroscopy (XPS): Recent developments and challenges. *Appl. Surf. Sci. Adv.* **2022**, *12*, 100332. [CrossRef]
16. Sun, B.; Zhang, J.; Wang, M.; Yu, S.; Xu, Y.; Tian, S.; Gao, Z.; Xiao, D.; Liu, G.; Zhou, W.; et al. Valorization of waste biodegradable polyester for methyl methacrylate production. *Nat. Sustain.* **2023**, *6*, 712–719. [CrossRef]
17. Xu, X.; Lan, T.; Zhao, G.; Nie, Q.; Jiang, F.; Lu, Y. Interface-hydroxyl enabling methanol steam reforming toward CO-free hydrogen production over inverse ZrO_2/Cu catalyst. *Appl. Catal. B Environ.* **2023**, *334*, 122839. [CrossRef]
18. Zhou, B.; Ma, Y.; Ou, P.; Ye, Z.; Li, X.-Y.; Vanka, S.; Ma, T.; Sun, H.; Wang, P.; Zhou, P.; et al. Light-driven synthesis of C_2H_6 from CO_2 and H_2O on a bimetallic AuIr composite supported on InGaN nanowires. *Nat. Catal.* **2023**, *6*, 987–995. [CrossRef]
19. Zhang, J.; Su, B.-J.; Wu, K.-H.; Xia, Q.; Knibbe, R.; Gentle, I. Low-coordinated surface nickel oxide as electrocatalyst for efficient water oxidation. *J. Catal.* **2024**, *429*, 115278. [CrossRef]
20. Gao, H.; Jiang, Y.; Chen, R.; Dong, C.-L.; Huang, Y.-C.; Ma, M.; Shi, Z.; Liu, J.; Zhang, Z.; Qiu, M.; et al. Alloyed Pt Single-Atom Catalysts for Durable PEM Water Electrolyzer. *Adv. Funct. Mater.* **2023**, *33*, 2214795. [CrossRef]
21. Huang, Q.; Xia, G.-J.; Huang, B.; Xie, D.; Wang, J.; Wen, D.; Lin, D.; Xu, C.; Gao, L.; Wu, Z.; et al. Activating lattice oxygen by a defect-engineered Fe_2O_3–CeO_2 nano-heterojunction for efficient electrochemical water oxidation. *Energy Environ. Sci.* **2024**, *17*, 5260–5272. [CrossRef]
22. Fedorov, A.Y.; Bukhtiyarov, A.V.; Panafidin, M.A.; Prosvirin, I.P.; Zubavichus, Y.V.; Bukhtiyarov, V.I. Thermally Induced Surface Structure and Morphology Evolution in Bimetallic Pt-Au/HOPG Nanoparticles as Probed Using XPS and STM. *Nanomaterials* **2024**, *14*, 57. [CrossRef]
23. Horrell, B.A.; Cocke, D.L. Application of Ion-Scattering Spectroscopy to Catalyst Characterization. *Catal. Rev.* **1987**, *29*, 447–491. [CrossRef]
24. Smith, D.P. Scattering of Low-Energy Noble Gas Ions from Metal Surfaces. *J. Appl. Phys.* **1967**, *38*, 340–347. [CrossRef]
25. Brongersmal, H.H.; Mu, P.M. Analysis of the outermost atomic layer of a surface by low-energy ion scattering. *Surf. Sci.* **1973**, *35*, 393–412. [CrossRef]
26. Brongersma, H.H.; Draxler, M.; de Ridder, M.; Bauer, P. Surface composition analysis by low-energy ion scattering. *Surf. Sci. Rep.* **2007**, *62*, 63–109. [CrossRef]
27. Cushman, C.V.; Brüner, P.; Zakel, J.; Major, G.H.; Lunt, B.M.; Smith, N.J.; Grehl, T.; Linford, M.R. Low energy ion scattering (LEIS). A practical introduction to its theory, instrumentation, and applications. *Anal. Methods* **2016**, *8*, 3419–3439. [CrossRef]
28. ter Veen, H.R.J.; Kim, T.; Wachs, I.E.; Brongersma, H.H. Applications of High Sensitivity-Low Energy Ion Scattering (HS-LEIS) in heterogeneous catalysis. *Catal. Today* **2009**, *140*, 197–201. [CrossRef]
29. Lang, R.; Xi, W.; Liu, J.-C.; Cui, Y.-T.; Li, T.; Lee, A.F.; Chen, F.; Chen, Y.; Li, L.; Li, L.; et al. Non defect-stabilized thermally stable single-atom catalyst. *Nat. Commun.* **2019**, *10*, 234. [CrossRef]
30. Hu, J.; Li, Y.; Zhen, Y.; Chen, M.; Wan, H. In situ FTIR and ex situ XPS/HS-LEIS study of supported Cu/Al_2O_3 and Cu/ZnO catalysts for CO_2 hydrogenation. *Chin. J. Catal.* **2021**, *42*, 367–375. [CrossRef]
31. Caporali, S.; Pedio, M.; Chiappe, C.; Pomelli, C.S.; Acres, R.G.; Bardi, U. Surface study of metal-containing ionic liquids by means of photoemission and absorption spectroscopies. *Surf. Sci.* **2016**, *648*, 360–365. [CrossRef]
32. Hemmeter, D.; Kremitzl, D.; Schulz, P.S.; Wasserscheid, P.; Maier, F.; Steinrück, H.-P. The Buoy Effect: Surface Enrichment of a Pt Complex in IL Solution by Ligand Design. *Chem.–A Eur. J.* **2023**, *29*, e202203325. [CrossRef]
33. Hemmeter, D.; Paap, U.; Maier, F.; Steinrück, H.-P. Structure and Surface Behavior of Rh Complexes in Ionic Liquids Studied Using Angle-Resolved X-ray Photoelectron Spectroscopy. *Catalysts* **2023**, *13*, 871. [CrossRef]
34. Hemmeter, D.; Paap, U.; Taccardi, N.; Mehler, J.; Schulz, P.; Wasserscheid, P.; Maier, F.; Steinrück, H.P. Formation and Surface Behavior of Pt and Pd Complexes with Ligand Systems Derived from Nitrile-functionalized Ionic Liquids Studied by XPS. *ChemPhysChem* **2023**, *24*, e202200391. [CrossRef]

35. Ma, W.; Fan, W.; Li, Q.; Zhang, H.; Zhu, K.; Sun, C.; Wang, L.; Zong, X. Chloroplast-mimicking nanoreactor for enhanced CO_2 electrocatalysis. *Sci. Bull.* **2024**. [CrossRef]
36. Cui, Y.; Wu, Y.; Dai, W. XPS Analysis of Semiconductor GaN with Different Anodes. *J. Fudan Univ. Nat. Sci.* **2023**, *62*, 9–15. [CrossRef]
37. Bure, T.R.; Renault, O.; Nolot, E.; Lardin, T.; Robert-Goumet, C.; Pauly, N. Assessing advanced methods in XPS and HAXPES for determining the thicknesses of high-k oxide materials: From ultra-thin layers to deeply buried interfaces. *Appl. Surf. Sci.* **2023**, *609*, 155317. [CrossRef]
38. Vanleenhove, A.; Hoflijk, I.; Zborowski, C.; Vaesen, I.; Artyushkova, K.; Conard, T. High-energy X-ray photoelectron spectroscopy spectra of TiO_2 measured by Cr Kα. *Surf. Sci. Spectra* **2022**, *29*, 014017. [CrossRef]
39. Zborowski, C.; Conard, T.; Vanleenhove, A.; Hoflijk, I.; Vaesen, I. Reference survey spectra of elemental solid measured with Cr Kα photons as a tool for Quases analysis (1): Transition metals period 4 elements (Sc, Ti, V, Cr, Mn, Fe, Co, Ni, Cu, Zn). *Surf. Sci. Spectra* **2022**, *29*, 024002. [CrossRef]
40. Matsuo, J.; Toyoda, N.; Akizuki, M.; Yamada, I. Sputtering of elemental metals by Ar cluster ions. *Nucl. Instrum. Methods Phys. Res. Sect. B Beam Interact. Mater. At.* **1997**, *121*, 459–463. [CrossRef]
41. Yamada, I. Historical milestones and future prospects of cluster ion beam technology. *Appl. Surf. Sci.* **2014**, *310*, 77–88. [CrossRef]
42. Popok, V.N.; Barke, I.; Campbell, E.E.B.; Meiwes-Broer, K.-H. Cluster–surface interaction: From soft landing to implantation. *Surf. Sci. Rep.* **2011**, *66*, 347–377. [CrossRef]
43. Yamada, I.; Matsuo, J.; Toyoda, N.; Aoki, T.; Seki, T. Progress and applications of cluster ion beam technology. *Curr. Opin. Solid State Mater. Sci.* **2015**, *19*, 12–18. [CrossRef]
44. Aoki, T. Molecular dynamics simulations of cluster impacts on solid targets: Implantation, surface modification, and sputtering. *J. Comput. Electron.* **2014**, *13*, 108–121. [CrossRef]
45. Zemek, J.; Jiricek, P.; Houdkova, J.; Artemenko, A.; Jelinek, M. Diamond-like carbon and nanocrystalline diamond film surfaces sputtered by argon cluster ion beams. *Diam. Relat. Mater.* **2016**, *68*, 37–41. [CrossRef]
46. Hu, Q.; Tan, R.; Yao, W.; Cui, Y.; Li, J.; Song, W. Preparation and X-ray photoelectron spectroscopic characterization of Sn-doped C12A7:e− electride nanoparticles. *Appl. Surf. Sci.* **2020**, *508*, 145244. [CrossRef]
47. Zhang, L.; Cui, Y.; Yang, F.; Zhang, Q.; Zhang, J.; Cao, M.; Dai, W.-L. Electroless-hydrothermal construction of nickel bridged nickel sulfide@mesoporous carbon nitride hybrids for highly efficient noble metal-free photocatalytic H_2 production. *J. Mater. Sci. Technol.* **2020**, *45*, 176–186. [CrossRef]
48. Zhang, H.; Gu, H.; Huang, Y.; Wang, X.; Gao, L.; Li, Q.; Li, Y.; Zhang, Y.; Cui, Y.; Gao, R.; et al. Rational design of covalent organic frameworks/$NaTaO_3$ S-scheme heterostructure for enhanced photocatalytic hydrogen evolution. *J. Colloid Interface Sci.* **2024**, *664*, 916–927. [CrossRef]
49. Hueso, J.L.; Martínez-Martínez, D.; Caballero, A.; González-Elipe, A.R.; Mun, B.S.; Salmerón, M. Near-ambient X-ray photoemission spectroscopy and kinetic approach to the mechanism of carbon monoxide oxidation over lanthanum substituted cobaltites. *Catal. Commun.* **2009**, *10*, 1898–1902. [CrossRef]
50. Bentrup, U. Combining in situ characterization methods in one set-up: Looking with more eyes into the intricate chemistry of the synthesis and working of heterogeneous catalysts. *Chem. Soc. Rev.* **2010**, *39*, 4718–4730. [CrossRef]
51. Zhao, C.-X.; Liu, J.-N.; Li, B.-Q.; Ren, D.; Chen, X.; Yu, J.; Zhang, Q. Multiscale Construction of Bifunctional Electrocatalysts for Long-Lifespan Rechargeable Zinc–Air Batteries. *Adv. Funct. Mater.* **2020**, *30*, 2003619. [CrossRef]
52. Trotochaud, L.; Head, A.R.; Karslıoğlu, O.; Kyhl, L.; Bluhm, H. Ambient pressure photoelectron spectroscopy: Practical considerations and experimental frontiers. *J. Phys. Condens. Matter* **2017**, *29*, 053002. [CrossRef]
53. Zhong, L.; Chen, D.; Zafeiratos, S. A mini review of in situ near-ambient pressure XPS studies on non-noble, late transition metal catalysts. *Catal. Sci. Technol.* **2019**, *9*, 3851–3867. [CrossRef]
54. Isaacs, M.; Davies-Jones, J.; Davies, P.; Guan, S.; Lee, R.; Morgan, D.; Palgrave, R. Advanced XPS Characterization: XPS-based multi-technique analyses for comprehensive understanding of functional materials. *Mater. Chem. Front.* **2021**, *5*, 7931–7963. [CrossRef]
55. Li, S.; Xu, Y.; Chen, Y.; Li, W.; Lin, L.; Li, M.; Deng, Y.; Wang, X.; Ge, B.; Yang, C.; et al. Tuning the Selectivity of Catalytic Carbon Dioxide Hydrogenation over Iridium/Cerium Oxide Catalysts with a Strong Metal–Support Interaction. *Angew. Chem. Int. Ed.* **2017**, *56*, 10761–10765. [CrossRef]
56. Zhang, G.; Fan, G.; Yang, L.; Li, F. Tuning surface-interface structures of ZrO_2 supported copper catalysts by in situ introduction of indium to promote CO_2 hydrogenation to methanol. *Appl. Catal. A Gen.* **2020**, *605*, 117805. [CrossRef]
57. Dong, C.; Gao, Z.; Li, Y.; Peng, M.; Wang, M.; Xu, Y.; Li, C.; Xu, M.; Deng, Y.; Qin, X.; et al. Fully exposed palladium cluster catalysts enable hydrogen production from nitrogen heterocycles. *Nat. Catal.* **2022**, *5*, 485–493. [CrossRef]
58. Zhang, X.; Zhang, M.; Deng, Y.; Xu, M.; Artiglia, L.; Wen, W.; Gao, R.; Chen, B.; Yao, S.; Zhang, X.; et al. A stable low-temperature H_2-production catalyst by crowding Pt on α-MoC. *Nature* **2021**, *589*, 396–401. [CrossRef]
59. Wang, H.; Fan, S.; Guo, S.; Wang, S.; Qin, Z.; Dong, M.; Zhu, H.; Fan, W.; Wang, J. Selective conversion of CO_2 to isobutane-enriched C4 alkanes over InZrOx-Beta composite catalyst. *Nat. Commun.* **2023**, *14*, 2627. [CrossRef]
60. Yang, H.; Chen, Y.; Cui, X.; Wang, G.; Cen, Y.; Deng, T.; Yan, W.; Gao, J.; Zhu, S.; Olsbye, U.; et al. A Highly Stable Copper-Based Catalyst for Clarifying the Catalytic Roles of Cu^0 and Cu^+ Species in Methanol Dehydrogenation. *Angew. Chem. Int. Ed.* **2018**, *57*, 1836–1840. [CrossRef]

61. Zhao, Z.; Gao, G.; Xi, Y.; Wang, J.; Sun, P.; Liu, Q.; Yan, W.; Cui, Y.; Jiang, Z.; Li, F. Selective and stable upgrading of biomass-derived furans into plastic monomers by coupling homogeneous and heterogeneous catalysis. *Chem* **2022**, *8*, 1034–1049. [CrossRef]
62. Jiao, Z.; Shang, M.; Liu, J.; Lu, G.; Wang, X.; Bi, Y. The charge transfer mechanism of Bi modified TiO_2 nanotube arrays: TiO_2 serving as a "charge-transfer-bridge". *Nano Energy* **2017**, *31*, 96–104. [CrossRef]
63. Low, J.; Dai, B.; Tong, T.; Jiang, C.; Yu, J. In Situ Irradiated X-ray Photoelectron Spectroscopy Investigation on a Direct Z-Scheme TiO_2/CdS Composite Film Photocatalyst. *Adv. Mater.* **2019**, *31*, 1807920. [CrossRef] [PubMed]
64. Wang, L.; Cheng, B.; Zhang, L.; Yu, J. In situ Irradiated XPS Investigation on S-Scheme TiO_2@$ZnIn_2S_4$ Photocatalyst for Efficient Photocatalytic CO_2 Reduction. *Small* **2021**, *17*, e2103447. [CrossRef]
65. Filippov, T.N.; Kovalevskiy, N.S.; Solovyeva, M.I.; Chetyrin, I.A.; Prosvirin, I.P.; Lyulyukin, M.N.; Selishchev, D.S.; Kozlov, D.V. In situ XPS data for the uranyl-modified oxides under visible light. *Data Brief* **2018**, *19*, 2053–2060. [CrossRef] [PubMed]
66. Sezen, H.; Suzer, S. XPS for chemical- and charge-sensitive analyses. *Thin Solid Film.* **2013**, *534*, 1–11. [CrossRef]
67. Sezen, H.; Rockett, A.A.; Suzer, S. XPS Investigation of a CdS-Based Photoresistor under Working Conditions: Operando–XPS. *Anal. Chem.* **2012**, *84*, 2990–2994. [CrossRef]
68. Costantini, R.; Grazioli, C.; Cossaro, A.; Floreano, L.; Morgante, A.; Dell'Angela, M. Pump–Probe X-ray Photoemission Reveals Light-Induced Carrier Accumulation in Organic Heterojunctions. *J. Phys. Chem. C* **2020**, *124*, 26603–26612. [CrossRef]
69. Zhang, F.; Li, Y.; Ding, B.; Shao, G.; Li, N.; Zhang, P. Electrospinning Photocatalysis Meet In Situ Irradiated XPS: Recent Mechanisms Advances and Challenges. *Small* **2023**, *19*, 2303867. [CrossRef]
70. Mu, C.; Lv, C.; Meng, X.; Sun, J.; Tong, Z.; Huang, K. In Situ Characterization Techniques Applied in Photocatalysis: A Review. *Adv. Mater. Interfaces* **2023**, *10*, 2201842. [CrossRef]
71. Gu, H.; Zhang, H.; Wang, X. Robust construction of CdSe nanorods@Ti_3C_2 MXene nanosheet for superior photocatalytic H_2 evolution. *Appl. Catal. B Environ. Int. J. Devoted Catal. Sci. Its Appl.* **2023**, *328*, 122537. [CrossRef]
72. Wang, H.; Wang, F.; Zhang, S.; Shen, J.; Zhu, X.; Cui, Y.; Li, P.; Lin, C.; Li, X.; Xiao, Q.; et al. Ice-Templated Synthesis of Atomic Cluster Cocatalyst with Regulable Coordination Number for Enhanced Photocatalytic Hydrogen Evolution. *Adv. Mater.* **2024**, *36*, 2400764. [CrossRef]
73. Huang, Y.; Gu, H.; Zhang, H.; Wang, X.; Gao, L.; Cui, Y.; Zong, B.; Li, H.; Dai, W.-L. Synergistic V–Nb Sites Modulate Selective Alkene Epoxidation with In Situ Photogenerated H_2O_2 over COF@MXene Heterostructures. *ACS Catal.* **2024**, *14*, 12541–12550. [CrossRef]
74. Li, Y.; Wang, L.; Zhang, F.; Zhang, W.; Shao, G.; Zhang, P. Detecting and Quantifying Wavelength-Dependent Electrons Transfer in Heterostructure Catalyst via In Situ Irradiation XPS. *Adv. Sci.* **2023**, *10*, e2205020. [CrossRef] [PubMed]
75. Li, Y.; Zhang, Y.; Hou, R.; Ai, Y.; Cai, M.; Shi, Z.; Zhang, P.; Shao, G. Revealing electron numbers-binding energy relationships in heterojunctions via in-situ irradiated XPS. *Appl. Catal. B Environ. Energy* **2024**, *356*, 124223. [CrossRef]
76. Greczynski, G.; Hultman, L. A step-by-step guide to perform X-ray photoelectron spectroscopy. *J. Appl. Phys.* **2022**, *132*, 011101. [CrossRef]
77. Major, G.H.; Avval, T.G.; Moeini, B.; Pinto, G.; Shah, D.; Jain, V.; Carver, V.; Skinner, W.; Gengenbach, T.R.; Easton, C.D.; et al. Assessment of the frequency and nature of erroneous X-ray photoelectron spectroscopy analyses in the scientific literature. *J. Vac. Sci. Technol. A* **2020**, *38*, 061204. [CrossRef]
78. Major, G.H.; Pinder, J.W.; Austin, D.E.; Baer, D.R.; Castle, S.L.; Čechal, J.; Clark, B.M.; Cohen, H.; Counsell, J.D.P.; Herrera-Gomez, A.; et al. Perspective on improving the quality of surface and material data analysis in the scientific literature with a focus on X-ray photoelectron spectroscopy (XPS). *J. Vac. Sci. Technol. A* **2023**, *41*, 038501. [CrossRef]
79. Andrade, P.H.M.; Volkringer, C.; Loiseau, T.; Tejeda, A.; Hureau, M.; Moissette, A. Band gap analysis in MOF materials: Distinguishing direct and indirect transitions using UV–vis spectroscopy. *Appl. Mater. Today* **2024**, *37*, 102094. [CrossRef]
80. Rotonnelli, B.; Fernandes, M.-S.D.; Bournel, F.; Gallet, J.-J.; Lassalle-Kaiser, B. In situ/operando X-ray absorption and photoelectron spectroscopies applied to water-splitting electrocatalysis. *Curr. Opin. Electrochem.* **2023**, *40*, 101314. [CrossRef]
81. Weingarth, D.; Foelske-Schmitz, A.; Wokaun, A.; Kötz, R. In situ electrochemical XPS study of the Pt/[EMIM][BF_4] system. *Electrochem. Commun.* **2011**, *13*, 619–622. [CrossRef]
82. Ogletree, D.F.; Bluhm, H.; Lebedev, G.; Fadley, C.S.; Hussain, Z.; Salmeron, M. A differentially pumped electrostatic lens system for photoemission studies in the millibar range. *Rev. Sci. Instrum.* **2002**, *73*, 3872–3877. [CrossRef]